HHS Public Access

Author manuscript

J Biol Chem. Author manuscript; available in PMC 2017 September 18.

Published in final edited form as:

J Biol Chem. 2002 May 24; 277(21): 19056–19063. doi:10.1074/jbc.M110960200.

Identification by Site-directed Mutagenesis of Residues Involved in Ligand Recognition and Activation of the Human A_3 Adenosine Receptor

Zhan-Guo Gao[‡,§], **Aishe Chen**[‡], **Dov Barak**[‡,§,¶], **Soo-Kyung Kim**[‡], **Christa E. Müller**[‖], and **Kenneth A. Jacobson**[‡,**]

[‡]Molecular Recognition Section, Laboratory of Bioorganic Chemistry, NIDDK, National Institutes of Health, Bethesda, Maryland 20892

[‖]Pharmaceutical Institute, University of Bonn, Kreuzbergweg 26, D-53115 Bonn, Germany

Abstract

Ligand recognition has been extensively explored in G protein-coupled A_1, A_{2A}, and A_{2B} adenosine receptors but not in the A_3 receptor, which is cerebroprotective and cardioprotective. We mutated several residues of the human A_3 adenosine receptor within transmembrane domains 3 and 6 and the second extracellular loop, which have been predicted by previous molecular modeling to be involved in the ligand recognition, including His^{95}, Trp^{243}, Leu^{244}, Ser^{247}, Asn^{250}, and Lys^{152}. The N250A mutant receptor lost the ability to bind both radiolabeled agonist and antagonist. The H95A mutation significantly reduced affinity of both agonists and antagonists. In contrast, the K152A (EL2), W243A (6.48), and W243F (6.48) mutations did not significantly affect the agonist binding but decreased antagonist affinity by ~3–38-fold, suggesting that these residues were critical for the high affinity of A_3 adenosine receptor antagonists. Activation of phospholipase C by wild type (WT) and mutant receptors was measured. The A_3 agonist 2-chloro-N^6-(3-iodobenzyl)-5′-*N*-methylcarbamoyladenosine stimulated phosphoinositide turnover in the WT but failed to evoke a response in cells expressing W243A and W243F mutant receptors, in which agonist binding was less sensitive to guanosine 5′-γ-thiotriphosphate than in WT. Thus, although not important for agonist binding, Trp^{243} was critical for receptor activation. The results were interpreted using a rhodopsin-based model of ligand-A_3 receptor interactions.

The physiological effects of extracellular adenosine are mediated by four G protein-coupled receptors (GPCRs),[1] *i.e.* A_1, A_{2A}, A_{2B}, and A_3 adenosine receptors. The A_3 adenosine receptor, which is the most recently identified adenosine receptor subtype (1, 2), is

[**]To whom correspondence should be addressed: Molecular Recognition Section, Laboratory of Bioorganic Chemistry, NIDDK, National Institutes of Health, Bldg. 8A, Rm. B1A-19, Bethesda, MD 20892-0810. Tel.: 301-496-9024; Fax: 301-480-8422; kajacobs@helix.nih.gov.

[§]Supported by Gilead Sciences, Foster City, CA.

[¶]On leave from the Israel Institute for Biological Research, Ness Ziona, Israel.

[1]The abbreviations used are: GPCR, G protein-coupled receptor; AB-MECA, N^6-(4-aminobenzyl)-5′-*N*-methylcarboxamidoadenosine; ADA, adenosine deaminase; CADO, 2-chloroadenosine; CGS15943, 5-amino-9-chloro-2-(2-furyl)-1,2,4-triazolo[1,5-*c*]quinazoline; Cl-IB-MECA, 2-chloro-N^6-(3-iodobenzyl)-5′-*N*-methylcarbamoyladenosine; GTPγS, guanosine 5′-γ-thiotriophosphate; IB-MECA, N^6-(3-iodobenzyl)-5′-*N*-methylcarboxamidoadenosine; MRS1939, (1′*R*,2′*R*,3′*S*,4′*R*,5′*S*)-4-{6-[(3-iodophenylmethyl)amino]purin-9-yl}-1-(methylaminocarbonyl)bicyclo[3.1.0] hexane-2,3-diol; MRS1898, (1′*R*,2′*R*,3′*S*,4′*R*,5′*S*)-4-{2-chloro-6-[(3-iodophenylmethyl)amino]purin-9-yl}-1-(methylaminocarbonyl)bicyclo [3.1.0]hexane-2,3-diol;

implicated in a variety of important physiological processes (3–5). Activation of A_3 adenosine receptors increases the release of inflammatory mediators, such as histamine, from rodent mast cells (6) and inhibits the production of tumor necrosis factor-α (2, 7). The activation of the A_3 adenosine receptor is also suggested to be involved in immunosuppression (8) and in the response to ischemia of the brain (9, 10) and heart (11). It is becoming increasingly apparent that agonists or antagonists of A_3 adenosine receptors have potential as therapeutic agents for the treatment of ischemic and inflammatory diseases (5, 8).

The development of agonists and antagonists for the A_3 receptors has so far been directed by traditional medicinal chemistry. The availability of genetic information promises to facilitate understanding of the drug-receptor interaction leading to the rational design of a potentially therapeutically important class of drugs. Molecular modeling may further rationalize observed interactions between the receptor and a ligand. Previously, models derived for GPCRs based on structural homology with bacteriorhodopsin (12–14) had been helpful in understanding and predicting drug-receptor interactions for a variety of receptors. The high resolution crystal structure of bovine rhodopsin has been determined recently (15), providing a detailed atomic description of a GPCR in an inactive conformation and a solid basis for modeling the structure of other rhodopsin-like GPCRs. Such models can be used to help rationalize many observations made on the relationships between the conserved residues and the functional coupling properties. Conservation of functionally important sequences or residues within a certain receptor family is generally considered as a basis for the molecular mechanism leading to the receptor activation in the various subtypes of this receptor family. However, considering the diversity of ligands for different receptors or for different subtypes of a certain receptor family, it has also been accepted that different receptor subtypes may have quite specific structural and functional characteristics.

The ligand-binding sites on the A_1, A_{2A}, and A_{2B} receptors have been characterized previously (16–20) using site-directed mutagenesis. However, the molecular basis for ligand recognition in the A_3 adenosine receptor remains largely unknown. Only very recently, we created a “neoceptor” and several constitutively active mutant human A_3 adenosine receptors by site-directed mutagenesis (21, 22), which provided new insight into the molecular recognition in the A_3 receptor. In order to provide additional insights into ligand-A_3 adenosine receptor interactions, site-directed mutagenesis was used to study the role of a number of residues in the transmembrane (TM) domains and the second extracellular loop (EL2, Fig. 1). The present study identified a number of residues essential for high affinity binding of agonist and/or antagonist, as well as the receptor activation process. The results were interpreted with the aid of a model of ligand-A_3 receptor interactions based on the high resolution crystal structure of bovine rhodopsin.

MRS1220, *N*-[9-chloro-2-(2-furanyl)[1,2,4]triazolo [1,5-c]quinazolin-5-yl]benzene-acetamide; NECA, 5′-*N*-ethylcarboxamido adenosine; PSB-11, 8-ethyl-4-methyl-2-phenyl-(8*R*)-4,5,7,8-tetrahydro-1*H*-imidazo[2.1-*i*]purin-5-one; PLC, phospholipase C; WT, wild type; TM, transmembrane.

EXPERIMENTAL PROCEDURES

Materials

The vector pcDNA3 was obtained from Invitrogen. Human A_3 adenosine receptor cDNA was provided by M. Atkinson, A. Townsend-Nicholson, and P. R. Schofield (Garvan Medical Institute, Sydney, Australia) and was subcloned in pcDNA3 as pcDNA3/hA_3R. All oligonucleotides used were synthesized by Bioserve Biotechnologies (Laurel, MD). [^{125}I]*N*^{6}-(4-Amino-3-iodobenzyl)adenosine-5′-*N*-methyluronamide ([^{125}I]I-AB-MECA; 2000 Ci/mmol) and [^{3}H]8-ethyl-4-methyl-2-phenyl-(8*R*)-4,5,7,8-tetrahydro-1*H*-imidazo[2.1-*i*]purin-5-one ([^{3}H]PSB-11) (23) were from Amersham Biosciences; myo-[^{3}H]inositol (20 Ci/mmol) was obtained from American Radiolabeled Chemicals (St. Louis, MO). 2-Chloro-*N*^{6}-(3-iodobenzyl)adenosine-5′-*N*-methyluronamide (Cl-IB-MECA) and GTPγS were from Sigma. MRS1898 was synthesized as described previously (24). All the enzymes used in this study were obtained from New England Biolabs (Beverly, MA). QuikChange™ site-directed mutagenesis kit was purchased from Stratagene (La Jolla, CA). A monoclonal antibody (12CA5) against a hemagglutinin epitope and adenosine deaminase (ADA) were obtained from Roche Diagnostics (Indianapolis, IN), and goat anti-mouse IgG antibody conjugated with horseradish peroxidase was from Sigma.

Numbering Scheme of GPCRs

For sequence alignments of selected regions of A_3 adenosine receptors and other GPCRs, the standardized numbering system of van Rhee and Jacobson (25) was used to identify residues in the transmembrane domains (TMs) of various receptors. Each residue is identified by two numbers as follows: the first corresponds to the TM in which it is located; the second indicates its position relative to a particular highly conserved residue in that helix, arbitrarily assigned to 50. For example, His3.37 is the histidine in TM3, located 13 residues before the conserved arginine R3.50; Trp(6.48) corresponds to Trp^{243}.

Molecular Modeling

Briefly, a model of the human A_3 receptor was built in homology to the recently published x-ray structure of bovine rhodopsin (15) as described (21) using the Sybyl 6.6 modeling package. The model included the seven TMs (built and minimized individually and then grouped to form a helical bundle by adding one at a time) and the second extracellular loop, EL2 (conformation was initially modeled according to the corresponding domain of rhodopsin including the Cys^{83}–Cys^{166} disulfide bond). Models of the ligands were constructed using the “Sketch Molecule” module of Sybyl. The ligands were minimized in Sybyl (using MOPAC calculated partial atomic charges) and were rigidly docked into the helical bundle using graphic manipulation coupled to continuous energy monitoring. Manual adjustments of ligand conformation were followed by additional minimization runs of up to 1500 steps, using the Tripos force field with Amber all-atom force parameters until the root mean square value of the conjugate gradient (CG) was <0.1 kcal/mol/Å. A fixed dielectric constant = 4.0 was used throughout these calculations.

Transient Expression of Wild Type (WT) and Mutant Receptors in COS-7 Cells

COS-7 cells (10^{-6}) were grown in 100-mm cell culture dishes containing Dulbecco's modified Eagle's medium supplemented with 10% fetal bovine serum, 100 units/ml penicillin, 100 μg/ml streptomycin, and 2 μmol/ml glutamine. After 24 h, cells were washed with phosphate-buffered saline (with calcium) and then transfected with plasmid DNA (10 μg/dish) using the DEAE-dextran method (26) for 1 h. The cells were then treated with 100 μM chloroquine for 3 h in culture medium and cultured for an additional 48 h at 37 ° C and 5% CO_2.

Membrane Preparation

After 48 h of transfection COS-7 cells were washed two times with phosphate-buffered saline (without calcium) and harvested by trypsinization. Harvested cells were homogenized using a Polytron homogenizer and then centrifuged at 16,000 × *g* for 20 min. The resulting pellet was resuspended in the 50 mM Tris·HCl buffer (pH 8.0) in the presence of 3 units/ml ADA and stored at −80 °C in aliquots. The protein concentration was determined by using the method of Bradford (27).

[^{125}I]I-AB-MECA Binding Assay

For the agonist binding assay (21), each tube contained 50 μl of membrane suspension (8–12 μg of protein), 25μl of [^{125}I]I-AB-MECA (for competition studies, final concentration 1.0 nM), and 25 μl of increasing concentrations of the test ligands in Tris·HCl buffer (50 mM, pH 8.0) containing 10 mM $MgCl_2$, 1 mM EDTA. For saturation analysis of [^{125}I]I-AB-MECA binding, concentrations ranging from 0.1 to 20 nM were used. K_d values of the radioligand were determined for all mutant receptors. Nonspecific binding was determined using 10 μM Cl-IB-MECA in buffer. The mixtures were incubated at 37 °C for 60 min. Binding reactions were terminated by filtration through Whatman GF/B filters under reduced pressure using a MT-24 cell harvester (Brandell, Gaithersburg, MD). Filters were washed three times with 9 ml of ice-cold buffer. Radioactivity was determined in a Beckman 5500B γ-counter.

Binding of the Radiolabeled, Selective Antagonist [^{3}H]PSB-11 to A_3 Adenosine Receptors

Membranes (80 μg of protein) were incubated with 8 nM [^{3}H]PSB-11 (23) at 25 °C in a total assay volume of 400 μl for 60 min). Nonspecific binding was measured in the presence of 10 μM Cl-IB-MECA. Binding reactions were terminated by filtration through Whatman GF/B filters under reduced pressure using a MT-24 cell harvester (Brandel, Gaithersburg, MD).

Inositol Phosphate Determination

The method used was similar to that of Harden *et al.* (28). About 24 h after transfection, the cells were harvested by trypsinization and grown in 6-well plates (~10^6 cells/well; Costar, Cambridge, MA) in Dulbecco's modified Eagle's culture medium supplemented with 2 μCi/ml myo-[^{3}H]inositol. After a 24-h labeling period, cells were preincubated in the presence of 3 units/ml ADA for 30 min at 37 °C with 10 mM LiCl and for 20 min at room temperature. The mixtures were swirled to ensure uniformity. Following the addition of the agonist Cl-IB-MECA, the cells were incubated for 30 min at 37 °C and 5% CO_2. The

supernatants were removed by aspiration, and 750 μl of cold 20 mM formic acid was added to each well. Cell extracts were collected after a 30-min incubation at 4 °C and neutralized with 250 μl of 60 mM NH_4OH. The inositol monophosphate fraction was then isolated by anion exchange chromatography (29). The content of each well was applied to a small anion exchange column (AG-1-X8; Bio-Rad) that had been pretreated with 15 ml of 0.1 M formic acid, 3 M ammonium formate, followed by 15 ml of water. The columns were then washed with 15 ml of a solution containing 5 mM sodium borate and 60 mM sodium formate. [^{3}H]Inositol phosphates were eluted twice with 5 ml of 0.1 M formic acid, 0.2 M ammonium formate, and radioactivity was quantified by liquid scintillation counting (LKB Wallace 1215 Rackbeta scintillation counter).

Statistical Analysis

Binding and functional parameters were calculated using the Prism software (GraphPAD, San Diego). IC_{50} values obtained from competition curves were converted to K_i values using the Cheng-Prusoff equation (30). Data were expressed as means ± S.E.

RESULTS

The A_3 receptor cDNAs were initially isolated from rat testis and rat brain cDNA libraries and later from other species (31, 32). Sequence alignments for selected transmembrane domains of four human adenosine receptor subtypes, sheep and rat A_3 receptors, and other GPCRs are shown in Fig. 2. The A_3 receptor exhibits the lowest degree of identity between species compared with other adenosine receptor subtypes (31, 32). The residues of the human A_3 adenosine receptor selected for mutation in this study are shown in boldface type. His^{95} (3.37) is conserved in A_3 receptors from various species including human, sheep and rat, and the corresponding residue in A_1 and A_{2A} adenosine receptor (Gln) has been studied (33, 34). Lys^{152} occurs in the second extracellular loop (EL2). Three residues in TM6 were mutated as follows: Trp^{243} (6.48), Ser^{247} (6.52; corresponding to His in human A_1 and A_{2A} receptors), and Asn^{250} (6.55). All of these residues were predicted in molecular modeling (21) to be involved in the ligand recognition in the A_3 adenosine receptor. By comparison, we also tested the role of Leu^{244} (6.49), which was not predicted to be involved in ligand recognition but was located one helical turn below Ser^{247}. Each of these residues was individually replaced with Ala or both Ala and Phe.

Ligand Binding Properties of the WT and Mutant Receptors

The affinity of a number of agonists and antagonists belonging to different chemical classes (Fig. 3) were tested in both WT and mutant receptors. As shown in Fig. 4, following the mutation of His^{95} to Ala, the affinity of the high affinity selective A_3 agonist, Cl-IB-MECA, decreased 26-fold. Similar to Cl-IB-MECA, the affinity of other agonists and antagonists with different structures was decreased by the H95A mutation (Table I). The affinity of most test ligands for the H95A mutant receptor was ~10–100-fold lower than that for the WT receptor, suggesting that this residue is important for ligand recognition in the A_3 adenosine receptor.

The Trp residue (6.48) is conserved among all four subtypes of adenosine receptors and a variety of other GPCRs (Fig. 3) and was proposed to be involved in ligand recognition in human A_3 adenosine receptors as predicted by molecular modeling. However, the replacement of this Trp by Ala or Phe did not influence the agonist binding affinity, as determined by saturation experiment using [^{125}I]I-AB-MECA. The displacement of [^{125}I]I-AB-MECA binding by five agonists, adenosine derivatives CADO, Cl-IB-MECA, and NECA; the rigid methanocarba derivative MRS1898 (24); and the xanthine riboside *N*-methyl-1,3-dibutylxanthine 7-β-D-ribofuronamide, was also not affected by mutation of Trp^{243}. The K_d value for [^{125}I]I-AB-MECA and K_i values for other agonists were summarized in Table I.

In contrast to the agonist binding, the binding affinity of the A_3 antagonist MRS1220 was diminished ~30-fold for the W243A mutant receptor (Fig. 5). Similar to MRS1220, other test antagonists also showed a marked decrease of binding affinity following the mutation of the Trp residue (Table I), suggesting the involvement, either directly or indirectly, of this residue in antagonist recognition.

Following the substitution of Leu^{244} or Ser^{247} with Ala, saturation experiments were carried out using [^{125}I]I-AB-MECA as a radioligand. Competitive binding of various ligands to human WT and mutant A_3 adenosine receptors demonstrated that the binding parameters for all the agonists and antagonists were only slightly affected (Table I). In contrast to L244A and S247A mutant receptors, the specific binding of [^{125}I]I-AB-MECA (1.0 nM) to the N250A mutant receptor was not detectable. In order to examine the effects of this mutation on antagonist binding, a radiolabeled A_3 antagonist [^{3}H]PSB-11 (8 nM, final concentration) was used in the experiment. Similar to the [^{125}I]I-AB-MECA binding, the mutation also resulted in a complete loss of high affinity [^{3}H]PSB-11 binding, suggesting that Asn^{250} is essential, either directly or indirectly, for ligand recognition in the human A_3 adenosine receptor. The proximity of this residue to the putative ligand binding site was predicted using the molecular modeling.

The Lys residue of EL2 was predicted to be involved in ligand recognition using a molecular model of the A_3 adenosine receptor (see below). Following the K152A mutation, the affinity of all the agonists tested was essentially unchanged; however, the antagonist affinity decreased 3–9-fold, suggestive of the possible involvement of this residue in antagonist recognition. The K_d and K_i values were summarized in Table I.

Agonist-induced Phosphoinositide Turnover in COS-7 Cells Expressing WT and Mutant Receptors

The A_3 adenosine receptor is coupled to G_i protein, whereas coupling to G_q protein is controversial, because some studies have shown that PLC activation by the A_3 adenosine receptor is prevented by pertussis toxin (3, 35). To test the activation of the WT and mutant receptors, we initially attempted to perform a cyclic AMP production assay in transfected COS-7 cells. However, we observed that both NECA and Cl-IB-MECA, at certain concentrations, induced an increase of cyclic AMP production in non-transfected COS-7 cells, suggesting the presence of an endogenous G_s-coupled adenosine receptor, possibly the A_{2B} adenosine receptor. In the same cell line, Cl-IB-MECA had no effect on basal

phosphoinositide turnover. Hence, to avoid interference by endogenous receptors, together with the fact that forskolin-stimulated adenylyl cyclase activity was only partly inhibited by A_3 receptor agonists as demonstrated elsewhere (36), the PLC assay was used in the determination of functional coupling of the WT and mutant receptors.

Fig. 6 demonstrated that Cl-IB-MECA induced accumulation of inositol phosphates in COS-7 cells expressing WT receptors in a concentration-dependent manner, with an EC_{50} of 260 ± 49 nM ($n = 3$). The H95A mutation did not influence the production of inositol phosphates significantly (EC_{50} = 224 ± 57 nM; $n = 3$) ($p > 0.05$ compared with WT). In contrast, no substantial stimulation of phosphoinositide turnover by Cl-IB-MECA was observed in COS-7 cells expressing W243A, W243F, and N250A mutant receptors. In the case of the L244A mutant receptor, Cl-IB-MECA could still stimulate PLC activity but with 36-fold decreased potency (EC_{50} = 9430 ± 2470 nM; $n = 3$). No enhancement in basal PLC activity was observed for these mutant receptors.

Effects of a Guanine Nucleotide, GTPγS, on Agonist Binding

To characterize further the interactions between WT and mutant receptors and G proteins, we initially tried to do a membrane binding assay using [^{35}S]GTPγS; however, the signal-to-noise ratio was quite low. Hence, the ability of WT and W243A and W243F mutant receptors to interact with G proteins was further evaluated by measuring the effects of GTPγS on binding of the agonist [^{125}I]I-AB-MECA and on agonist Cl-IB-MECA competition for [^{3}H]PSB-11 binding in membranes of COS-7 cells expressing WT and mutant receptors. As shown in Fig. 7, treatment with GTPγS reduced agonist binding. The inhibitory effect of this GTP analogue on agonist binding to W243A and W243F mutant receptors was less pronounced compared with that of WT receptors, consistent with the impaired ability of these mutant receptors to mediate inositol phosphate production in response to an A_3 agonist.

A GTP-induced shift of agonist competition for radiolabeled antagonist is another indicator of functional coupling between a receptor and G protein. In this study, we further observed the effect of GTPγS on the competition by agonist Cl-IB-MECA for binding of the antagonist [^{3}H]PSB-11 to WT and mutant receptors. The K_i values for Cl-IB-MECA in the absence and presence 100 μM GTPγS were 2.5 ± 0.4 and 7.4 ± 1.1 nM, respectively, in WT receptors. In W243F mutant receptors, the respective K_i values were 2.3 ± 0.2 and 3.2 ± 0.4 nM. Hence, the GTP analogue induced a 3-fold affinity decrease of Cl-IB-MECA in WT receptors, whereas in the W243F mutant receptor only a 1.4-fold decrease of affinity was observed, consistent with the impaired ability of agonist to activate PLC through this mutant receptor. In the case of the W243A mutant receptor, the agonist affinity shift could not be observed due to the extremely low affinity of this mutant receptor for the antagonist radioligand [^{3}H]PSB-11.

Molecular Modeling

Recently a human A_3 receptor model, including the seven transmembrane helical domains (TMs) and EL2, has been constructed (21) in homology to the x-ray structure of bovine rhodopsin (15). The model was used primarily to rationalize the observed effects of the

replacement of residue His^{272} (7.43) by glutamate on the receptor affinity toward A_3 agonists and antagonists. Through docking of the A_3 agonists and antagonists, we have initially defined the ligand binding environment to include side chains of residues Thr^{94} (3.36), His^{95} (3.37), Ser^{247} (6.52), Gln^{167} and Lys^{152} (EL2), and Ser^{271} (7.42) and Asn^{274} (7.45), and we suggested differences in the accommodation of agonists bearing different N^6 substituents. Thus, although the N^6 moiety of CADO was located within H-bonding distance from the amide oxygen of Trp^{243} and Oγ of Ser^{247} (2.76 Å and 2.51 Å, respectively), the N^6-benzyl substituent of IB-MECA appeared to interact with residues Phe^{182}, Ile^{186}, and Phe^{187} in TM5. The effect of this bulky N^6 substitution on the orientation of the bound agonist was to displace the respective N^6 substituent away from the amide oxygen of Trp^{243}. Consequently the 3′-hydroxy substituent of IB-MECA did not seem to interact with His^{272}, whereas such interactions could be observed with the corresponding substituents of CADO or NECA. In addition, the modeled interaction of the agonist N^6 moiety with Oγ–Ser^{247} seemed to orient the adenine ring for aromatic–aromatic interaction with the indole moiety of Trp^{243}. Although this model could be used successfully to formalize the concept of neoceptor with respect to the A_3 receptor–agonist interaction (21), further experimental evidence was needed especially for corroborating the putative interactions of the adenine moiety of the agonists.

In the present study ligand accommodation in the A_3-binding site was further examined by modeling adducts of the various agonists and antagonists (Table I) with mutant receptors carrying residue replacements at the putative binding site. The results indicated that although the overall positioning of the ligands within the A_3 helical bundle was consistent with pharmacological findings, the orientation of the adenine moiety with respect to TM3 and TM6 had to be adjusted. In the modified models of A_3–agonist complexes the N^6 moiety interacted with Asn^{250} instead of Ser^{247}, tilting the adenine ring away from the indole moiety of Trp^{243}. This adjustment did not seem to affect the relative positions of the ribose (or the methanocarba (24)) moieties of the different agonists. Fig. 8 shows a molecular model of the human A_3 adenosine receptor complex with the nonselective antagonist CGS15943, which is located in proximity to both Trp^{243} and His^{95}, of which mutation reduced antagonist affinity.

The effects of replacement of His^{95} were consistent with the model with the imidazole moiety adjacent to the 2-position of the agonist adenine ring. Yet, the interaction seemed to depend upon the precise juxtaposition of the ligand, because affinity of the H95A receptor toward I-AB-MECA was only 3-fold lower compared with that of the WT receptor, whereas for NECA the ratio was 14-fold. Although both ligands lacked substitution at the 2-position, I-AB-MECA was shifted toward TM5 (relative to NECA) and therefore its adenine ring was further removed from the residue at position 95. Whereas the 100-fold affinity decrease of the H95A receptor toward CADO could be attributed to interaction with the 2-chloro substituent, comparison of the relative affinities of MRS1898 and MRS1939 did not support such a conclusion (Table II). In addition, the 2-chloro substituent did not seem to contribute to the affinity of either MRS1898 or of Cl-IB-MECA toward the A_3 receptor (Table II). Thus, although the model could accommodate small substituents at the 2-position of the adenine ring, the specific role of the 2-chloro substituent, which appeared in many of the A_3 agonists, in binding to the receptor remains unclear.

DISCUSSION

In this study we used a combination of mutagenesis, radio-ligand binding, functional activity (PLC), and molecular modeling approaches in order to identify residues important for ligand recognition in the human A_3 adenosine receptor. A change in the binding affinity due to a mutation can be due to an indirect effect on receptor structure and does not necessarily prove that the residue in question directly interacts with the ligand.

The most deleterious of the mutations with respect to binding affinity and functional potency was N250A (6.55), indicating that Asn^{250} is crucially involved in either human A_3 adenosine receptor-ligand recognition or in maintaining receptor structure. This asparagine residue is conserved among all four subtypes of adenosine receptors and a variety of other G protein-coupled receptors. Consistent with the present result, the mutation of the corresponding residue in the human A_{2A} adenosine receptor (N253A) also caused a drastic decrease of the affinity for both agonists and antagonists (18).

Although less critically required for ligand binding, His^{95} (3, 37) contributed significantly to the binding of most ligands tested in the present study. In A_1 adenosine receptors (the residue at the homologous position is Gln), the mutation (Q92A) also demonstrated its critical role in ligand recognition (34). However, in the human A_{2A} adenosine receptor, the mutation of the corresponding residue into Ala (Q89A) increased both agonist and antagonist affinity (33). Similar to the results obtained here, Perlman *et al.* (37) have demonstrated in a site-directed mutagenesis study that the mutation of the corresponding residue in murine thyrotropin-releasing hormone receptor (N110A) also decreased agonist binding. Similar results have also been reported in a study of human D_2 dopamine receptors, in which the antagonist binding affinity was significantly diminished after the mutation of the corresponding residue (T119C) (38).

Interestingly, we have identified a mutant receptor W243A (6.48) that bound agonist strongly but was functionally inactive. The function of this conserved residue has been extensively studied in a variety of G protein-coupled receptors, and it is suggested that this residue plays a subtle role in receptor binding and activation. The importance of this Trp residue in GPCR function was first emphasized by the study of its effects in rhodopsin, in which this residue forms part of the retinal-binding pocket (39). In contrast to the results obtained here, the mutation of the equivalent Trp residue in the mouse δ-opioid receptor (40) impaired the binding of most ligands. In the rat AT_{1A} receptor, the mutation of the homologous residue (W253A) decreased agonist but not antagonist binding (41). In rat m3 muscarinic receptor, the corresponding W503F mutation decreased both agonist and antagonist binding; however, receptor activation was not affected. Consistent with the present study, the mutation of the corresponding residue in the murine thyrotropin-releasing hormone receptor (W279A) did not affect agonist binding (42).

The major consequence of the W243A and W243F mutations was functional inactivation of the A_3 receptor, indicating that Trp^{243} may play a pivotal role in receptor transduction of the signal. The diminished effects of a guanine nucleotide on agonist binding in the Trp^{243} mutant receptors indicated impairment of the coupling of the receptor to G protein.

Activation of GPCRs involves positive heterotropic, long range interactions between agonist- and G protein-binding sites, and several lines of evidence suggested that the movements of TM6 were critical in this process (43–45). Molecular modeling suggested that the Trp^{243} was in the binding pocket, where it might occupy a strategic position and might act as a switch in TM6-mediated structural transition from the resting to active state. It is possible that the replacement of this residue with Ala or Phe left the switch in the “off ” position, resulting in functional inactivation and uncoupling. The result also suggested that this conserved Trp residue did not play the same role in agonist binding and receptor activation.

A recent study (46) demonstrated that the W256A mutation of the homologous residue in the human B_2 bradykinin receptor resulted in a marked decrease of the affinity of nonpeptide antagonists but not agonists, which is in fair agreement with the present study. These results suggested that this conserved residue might be specifically involved in antagonist recognition in some GPCRs. By comparison, mutation of residue Leu^{244} (at a neighboring position to Trp^{243}) to Ala did not influence the antagonist binding. These insights may prove useful in future efforts to design A_3 receptor antagonists by a rational approach.

In the present study, the mutation of the serine residue (S247A) in the TM6 of the human A_3 adenosine receptor did not influence agonist binding and only slightly affected antagonist binding, which is consistent with the results from the mutagenesis study of the bovine A_1 adenosine receptor. The mutation of the corresponding residue (H251L) diminished antagonist binding ~4-fold, but agonist binding was essentially not affected (47). This result was also consonant with the results of mutation of the corresponding residue (H265A) in the human NK1 receptor, which decreased antagonist binding but did not affect the agonist binding (48). In contrast to these results, the corresponding H250A mutation in the human A_{2A} receptor diminished agonist and antagonist binding as well as receptor activation (18). In rat m3 muscarinic receptors, the binding of agonist and antagonist was also impaired by the homologous N507A mutation (49). Similarly, in the m3 receptor, the agonist binding was decreased after the homologous R283A mutation in the murine thyrotropin-releasing hormone receptor (42). These results suggested that the residue at this position contributed unequally in different receptors. It was also further suggested that different receptor subtypes or different receptors might have quite specific structural and functional characteristics.

It is interesting that the H95A mutation impaired agonist binding but not agonist-induced receptor activation, whereas the W243A mutation impaired functional coupling but did not diminish agonist affinity. The mutation of residue Leu^{244} (adjacent to Trp^{243}) to Ala resulted in nearly the same agonist binding affinity as that of the WT receptor, but the activation was only partly impaired, also suggesting the involvement in the receptor activation process. Clearly these residues contribute differently to ligand binding and receptor activation processes.

In the modified models of A_3–agonist complexes the ligands did not interact directly with residue Trp^{243}. Yet this residue is essential for receptor activation, suggesting that binding of agonist may induce reorientation of its side chain accompanying the receptor transition from an inactive to an active state. Unlike the case of agonists, residue Trp^{243} seemed to

participate in accommodation of antagonists, apparently through aromatic–aromatic interactions. This conclusion was based upon the differential effect on affinity toward antagonists upon replacement of Trp^{243} with Phe and Ala (Table I). According to the data from mutagenesis and from molecular modeling, the binding sites of A_3 agonists and antagonists mostly overlap. Thus, the lack of participation of Trp^{243} in agonist binding probably resulted from a different size and nature of the adenine ring as compared with the aromatic systems of the antagonists. According to the models, these differences seemed to account also for a better interaction of antagonists with residue His^{95} and with Lys^{152}.

The models of A_3-ligand complexes suggested that motion of the Trp^{243} side chain may be one of the primary molecular events taking place upon ligand binding. In the inactive (dark) conformation of rhodopsin the side chain of the analogous Trp^{256} was oriented along the TM6 helical axis and interacted with the ring moiety of retinal. If the Trp^{243} side chain were to adopt a somewhat similar orientation in the free A_3 receptor, its $C\eta^2$ would be within interaction distance from His^{95}. Upon binding, the Trp^{243} side chain rotated out of the way of the incoming ligand and assumed a new conformation to position the indole moiety adjacent to Phe^{239}. In this new conformation Trp^{243} did not interact directly with agonists, yet the aromatic–aromatic interaction with Phe^{239} may stabilize the active conformation of the receptor.

In conclusion, the binding modes of nucleoside agonists and non-nucleoside antagonists at human A_3 receptors are different. Residues needed for antagonist but not agonist binding include Tyr243 (6.48) and Lys152 (EL2). Residues needed for both antagonist and agonist binding include His95 (3.37), His272 (7.43), and Asn250 (6.55), which is critical. Furthermore, it is possible to separate the structural bases for binding and activation processes. Trp243 is required for activation of the receptor but not for binding of agonists.

Acknowledgments

We thank Dr. Neli Melman (NIDDK) for assistance in radioligand binding assays. We thank Dr. Ad IJzerman (Leiden/Amsterdam Center for Drug Research, Leiden, The Netherlands) for the gift of 4-methoxy-*N*-[3-(2-pyridinyl)-1-isoquinolinyl]benzamide, Dr. Kyeong Lee (NIDDK) for preparing MRS1898, and Dr. Bruce Liang (University of Pennsylvania, Philadelphia, PA) for helpful discussions. Proofreading and graphics by Kelly Soltysiak (NIDDK) is appreciated.

References

1. Zhou QY, Li C, Olah ME, Johnson RA, Stiles GL, Civelli O. Proc Natl Acad Sci U S A. 1992; 89:7432–7436. [PubMed: 1323836]
2. Salvatore SA, Tilley SL, Latour AM, Fletcher DS, Koller BH, Jacobson MA. J Biol Chem. 2000; 275:4429–4434. [PubMed: 10660615]
3. Olah ME, Stiles GL. Pharmacol Ther. 2000; 85:55–75. [PubMed: 10722120]
4. Fredholm BB, Arslan G, Halldner L, Kull B, Schulte G, Wasserman W. Naunyn-Schmiedeberg's Arch Pharmacol. 2000; 362:364–374. [PubMed: 11111830]
5. Linden J. Annu Rev Pharmacol Toxicol. 2001; 41:775–787. [PubMed: 11264476]
6. Ramkumar V, Stiles GL, Beaven MA, Ali H. J Biol Chem. 1993; 268:16887–16890. [PubMed: 8349579]
7. Sajjadi FG, Takabayashi K, Foster AC, Domingo RC, Firestein GS. J Immunol. 1996; 156:3435–3442. [PubMed: 8617970]
8. Kaiser SM, Quinn RJ. Drug Disc Today. 1999; 4:542–551.

9. von Lubitz DK, Lin RC, Popik P, Carter MF, Jacobson KA. Eur J Pharmacol. 1994; 263:59–67. [PubMed: 7821362]
10. von Lubitz DK, Ye W, McClellan J, Lin RC. Ann N Y Acad Sci. 1999; 890:93–106. [PubMed: 10668416]
11. Liang BT, Jacobson KA. Proc Natl Acad Sci U S A. 1998; 95:6995–6999. [PubMed: 9618527]
12. Pardo L, Ballesteros JA, Osman R, Weinstein H. Proc Natl Acad Sci U S A. 1992; 89:4009–4012. [PubMed: 1315046]
13. Hibert MF, Trumpp-Kallmeyer S, Hoflack J, Bruinvels A. Trends Pharmacol Sci. 1993; 14:7–12. [PubMed: 8095116]
14. Unger VM, Hargrave PA, Baldwin JM, Schertler GF. Nature. 1997; 389:203–206. [PubMed: 9296501]
15. Palczewski K, Kumasaka T, Hori T, Behnke CA, Motoshima H, Fox BA, Le Trong I, Teller DC, Okada T, Stenkamp TE, Yamamoto M, Miyano M. Science. 2000; 289:739–745. [PubMed: 10926528]
16. Barbhaiya H, McClain R, IJzerman AP, Rivkees SA. Mol Pharmacol. 1996; 50:1635–1642. [PubMed: 8967987]
17. Tucker AL, Robeva AS, Taylor HE, Holeton D, Bockner M, Lynch KR, Linden J. J Biol Chem. 1994; 269:27900–27906. [PubMed: 7961722]
18. Kim J, Wess J, van Rhee AM, Schoneberg T, Jacobson KA. J Biol Chem. 1995; 270:13987–13997. [PubMed: 7775460]
19. Gao ZG, Jiang Q, Jacobson KA, IJzerman AP. Biochem Pharmacol. 2000; 60:661–668. [PubMed: 10927024]
20. Beukers MW, den Dulk H, van Tilburg EW, Brouwer J, IJzerman AP. Mol Pharmacol. 2000; 58:1349–1356. [PubMed: 11093773]
21. Jacobson KA, Gao ZG, Chen A, Barak D, Kim SA, Lee K, Link A, van Rompaey P, van Calenbergh S, Liang BT. J Med Chem. 2001; 44:4125–4136. [PubMed: 11708915]
22. Chen A, Gao ZG, Barak D, Liang BT, Jacobson KA. Biochem Biophys Res Commun. 2001; 284:596–601. [PubMed: 11396942]
23. Müller CE, Diekmann M, Thorand M, Ozola V. Bioorg Med Chem Lett. 2001; 12:501–503.
24. Lee K, Ravi RG, Ji XD, Marquez VE, Jacobson KA. Bioorg Med Chem Lett. 2001; 11:1333–1337. [PubMed: 11392549]
25. Van Rhee AM, Jacobson KA. Drug Dev Res. 1996; 37:1–38. [PubMed: 21921973]
26. Cullen BR. Methods Enzymol. 1987; 152:684–704. [PubMed: 3657593]
27. Bradford MM. Anal Biochem. 1976; 72:248–254. [PubMed: 942051]
28. Harden TK, Hawkins PT, Stephens L, Boyer JL, Downes P. Biochem J. 1988; 252:583–593. [PubMed: 2843174]
29. Berridge MJ, Dawson RM, Downes CP, Heslop JP, Irvine RF. Biochem J. 1983; 212:473–482. [PubMed: 6309146]
30. Cheng Y, Prusoff WH. Biochem Pharmacol. 1973; 22:3099–3108. [PubMed: 4202581]
31. Olah ME, Stiles GL. Annu Rev Pharmacol Toxicol. 1995; 35:581–606. [PubMed: 7598508]
32. Salvatore CA, Jacobson MA, Taylor HE, Linden J, Johnson RG. Proc Natl Acad Sci U S A. 1993; 90:10365–10369. [PubMed: 8234299]
33. Jiang Q, van Rhee AM, Kim J, Yehle S, Wess J, Jacobson KA. Mol Pharmacol. 1996; 50:512–521. [PubMed: 8794889]
34. Rivkees SA, Barbhaiya H, IJzerman AP. J Biol Chem. 1999; 274:3617–3621. [PubMed: 9920910]
35. Abbracchio MP, Brambilla R, Ceruti S, Kim HO, von Lubitz DK, Jacobson KA, Cattabeni F. Mol Pharmacol. 1995; 48:1038–1045. [PubMed: 8848003]
36. Jacobson KA, Park KS, Jiang JL, Kim YC, Olah ME, Stiles GL, Ji XD. Neuropharmacology. 1997; 36:1157–1165. [PubMed: 9364471]
37. Perlman JH, Laakkonen L, Osman R, Gershengorn MC. J Biol Chem. 1994; 269:23383–23386. [PubMed: 8089099]
38. Javitch JA, Fu D, Chen J, Karlin A. Neuron. 1995; 14:825–831. [PubMed: 7718244]

39. Nakayama TA, Khorana HG. J Biol Chem. 1990; 265:15762–15769. [PubMed: 2144289]
40. Befort K, Tabbara L, Kling D, Maigret B, Kieffer BL. J Biol Chem. 1996; 271:10161–10168. [PubMed: 8626577]
41. Yamano Y, Ohyama K, Kikyo M, Sano T, Nakagomi Y, Inoue Y, Nakamura N, Morishima I, Guo DF, Hamakubo T, Inagami T. J Biol Chem. 1995; 270:14024–14030. [PubMed: 7775462]
42. Perlman JH, Laakkonen L, Osman R, Gershengorn MC. Mol Pharmacol. 1995; 47:480–484. [PubMed: 7700246]
43. Dunham TD, Farrens DL. J Biol Chem. 1999; 274:1683–16890. [PubMed: 9880548]
44. Mouledous L, Topham CM, Moisand C, Mollereau C, Meunier JC. Mol Pharmacol. 2000; 57:495–502. [PubMed: 10692489]
45. Gether U. Endocr Rev. 2000; 21:90–113. [PubMed: 10696571]
46. Marie J, Richard E, Pruneau D, Paquet JL, Siatka C, Larguier R, Poncé C, Vassault P, Groblewski T, Maigret B, Bonnafous JC. J Biol Chem. 2001; 276:41100–41111. [PubMed: 11495910]
47. Olah ME, Ren H, Ostrowski J, Jacobson KA, Stiles GL. J Biol Chem. 1992; 267:10764–10770. [PubMed: 1587851]
48. Zoffmann S, Gether U, Schwartz TW. FEBS Lett. 1993; 336:506–510. [PubMed: 7506676]
49. Bluml K, Mutschler E, Wess J. J Biol Chem. 1994; 269:18870–18876. [PubMed: 8034642]

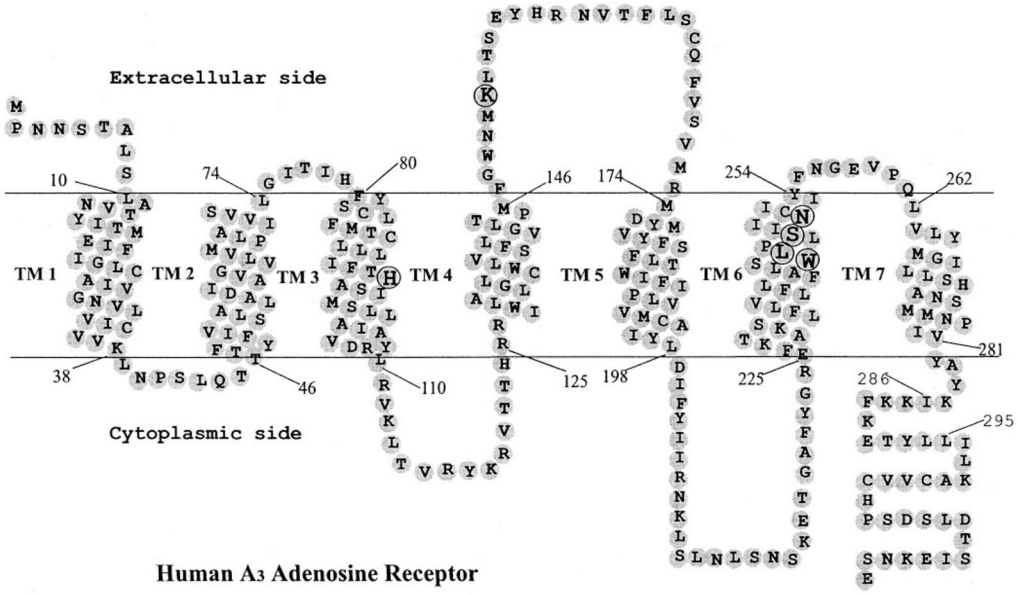

Fig. 1. Heptahelical diagram of the human A_3 adenosine receptor

The putative transmembrane domains were modified according to the high resolution rhodopsin model (15). Amino acids mutated in the present study are circled. Residues 286–295 correspond to an extra helical domain in rhodopsin, which is discontinuous from TM7.

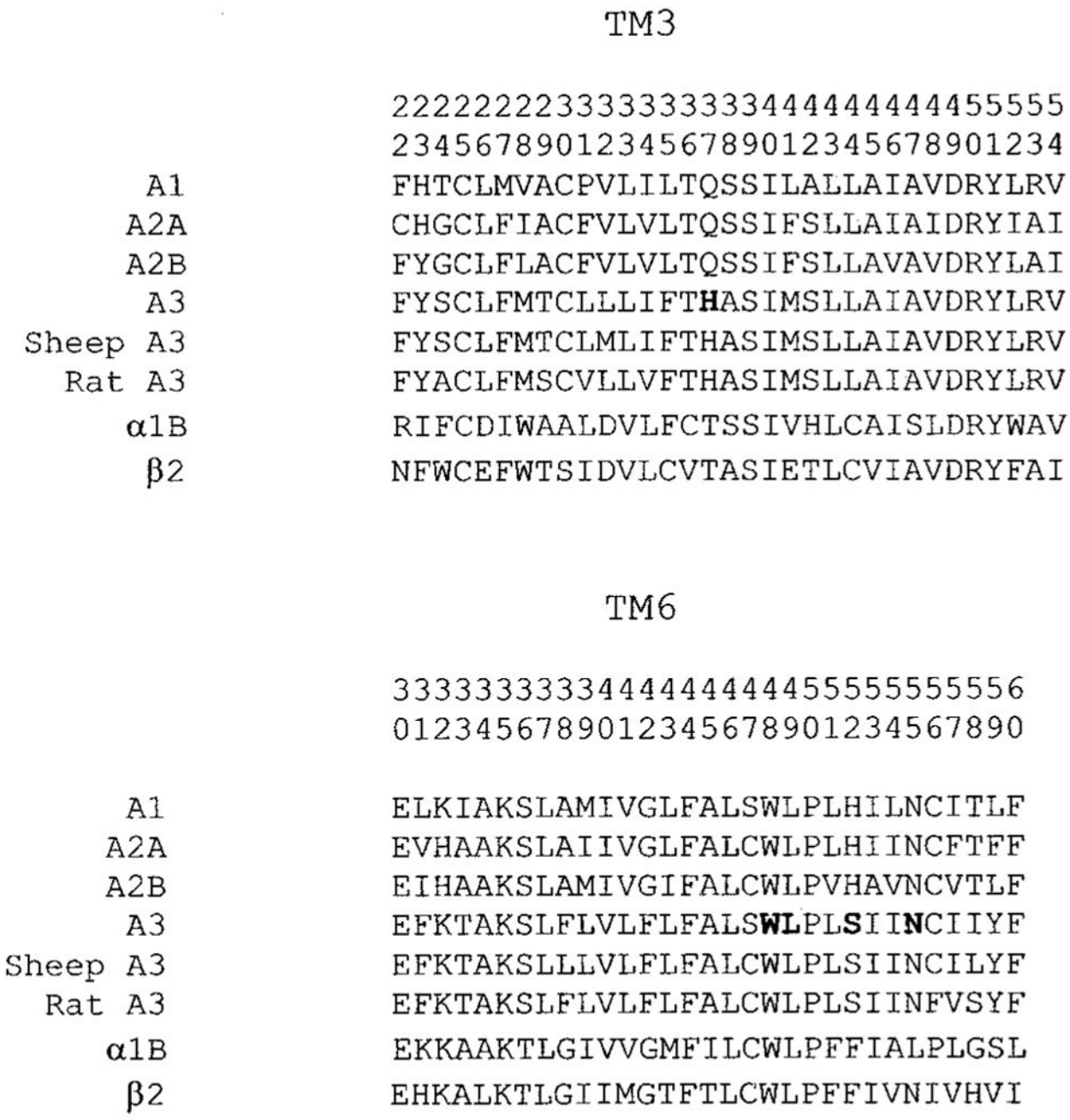

Fig. 2. Sequence alignments of selected regions of A_3 adenosine receptors and other G protein-coupled receptors

Residues mutated in this study are shown in *boldface type.* The standardized numbering system of van Rhee and Jacobson (25) was used to identify residues in the transmembrane domains (*TMs*) of various receptors. Each residue is identified by two numbers; the first corresponds to the TM in which it is located; the second indicates its position relative to the most conserved residue in that helix, arbitrarily assigned to 50. For example, H3.37 is the histidine in TM3, located 13 residues before the most conserved arginine R3.50; W6.48 corresponds to Trp^{243}.

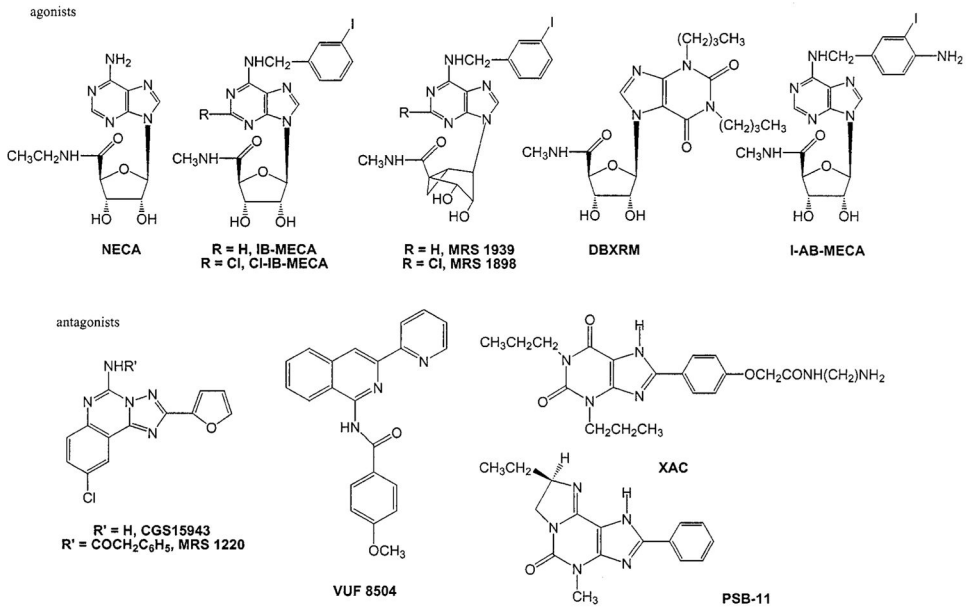

Fig. 3.
Chemical structures of ligands tested in this study.

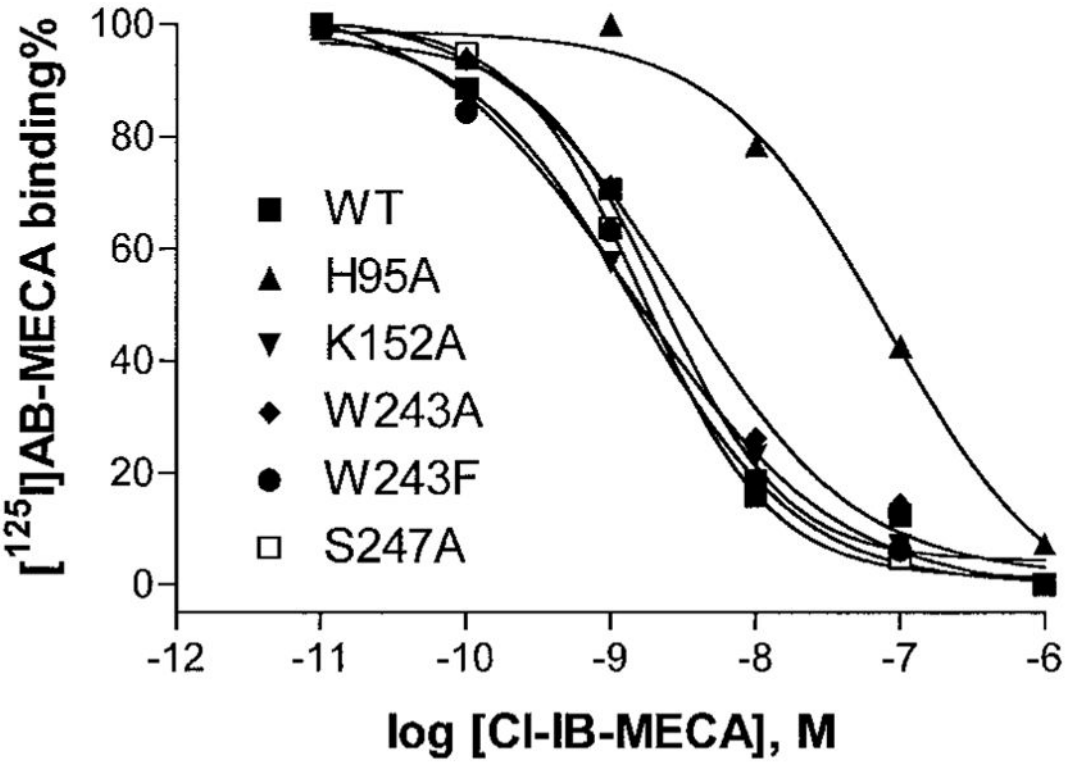

Fig. 4. Effects of mutations in TM3, TM6, and EL2 on the binding of A_3 agonist Cl-IB-MECA

The agonist radioligand [^{125}I]I-AB-MECA (1.0 nM) was used in the experiment. The data shown are from a representative example out of at least three independent experiments performed in duplicate.

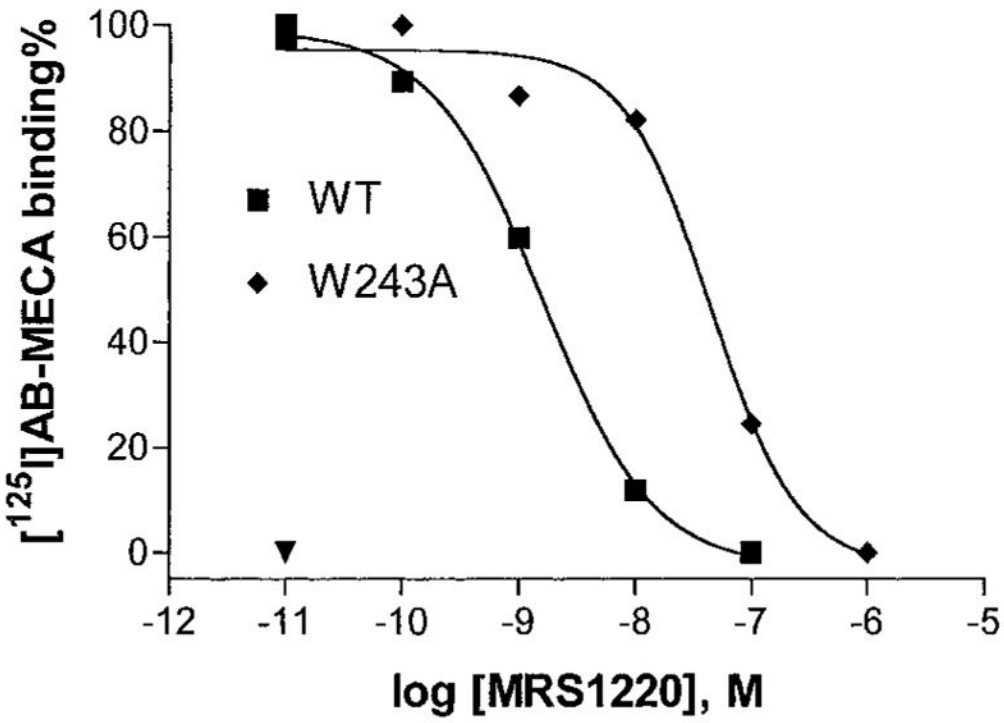

Fig. 5. Effects of the Trp mutation on the binding of A_3 antagonist MRS1220

The agonist radioligand [^{125}I]I-AB-MECA (1.0 nM) was used in the experiment. The data shown are from a representative example of at least three independent experiments performed in duplicate.

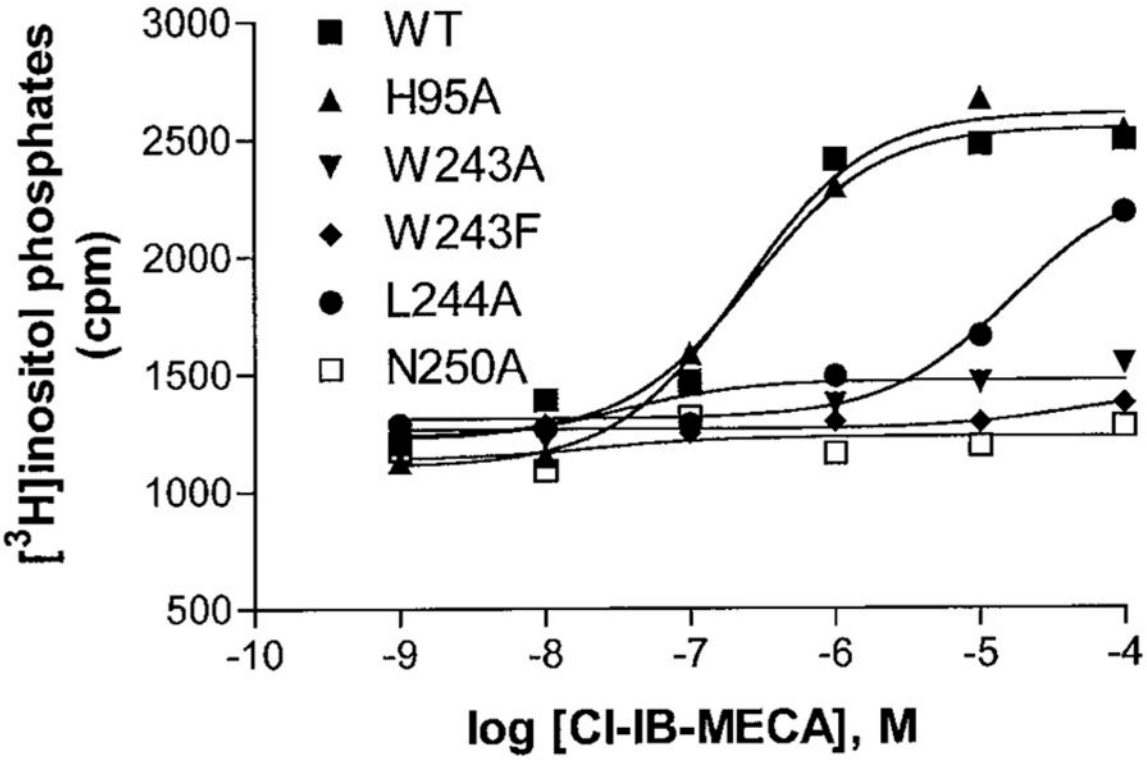

Fig. 6. Cl-IB-MECA induced phosphoinositide turnover in COS-7 cells expressing WT and mutant human A_3 adenosine receptors

Receptors were transiently expressed in COS-7 cells and used 48 h after transfection. The data shown are from a representative example of three independent experiments.

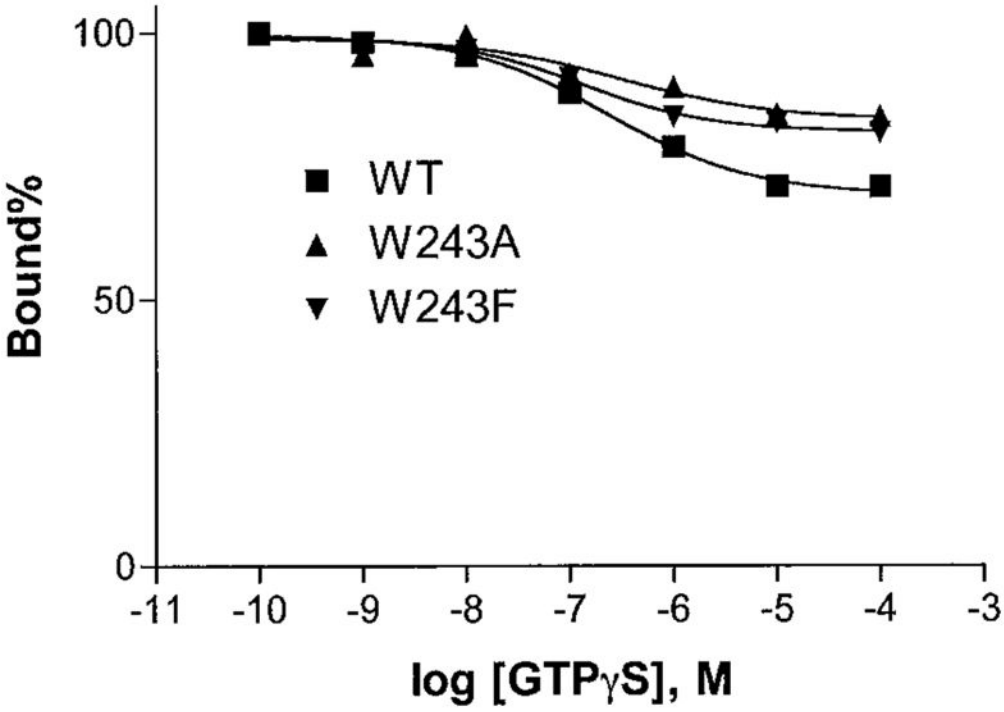

Fig. 7. Effects of GTP analogue on A_3 receptor binding

Shown are the effects of increasing concentrations of GTPγS on binding of the agonist radioligand [^{125}I]I-AB-MECA (1.0 nM) to membranes from COS-7 cells expressing WT and mutant receptors. Results are expressed as percent of binding determined in the absence of GTPγS and are shown as means of values obtained from three experiments performed in duplicate.

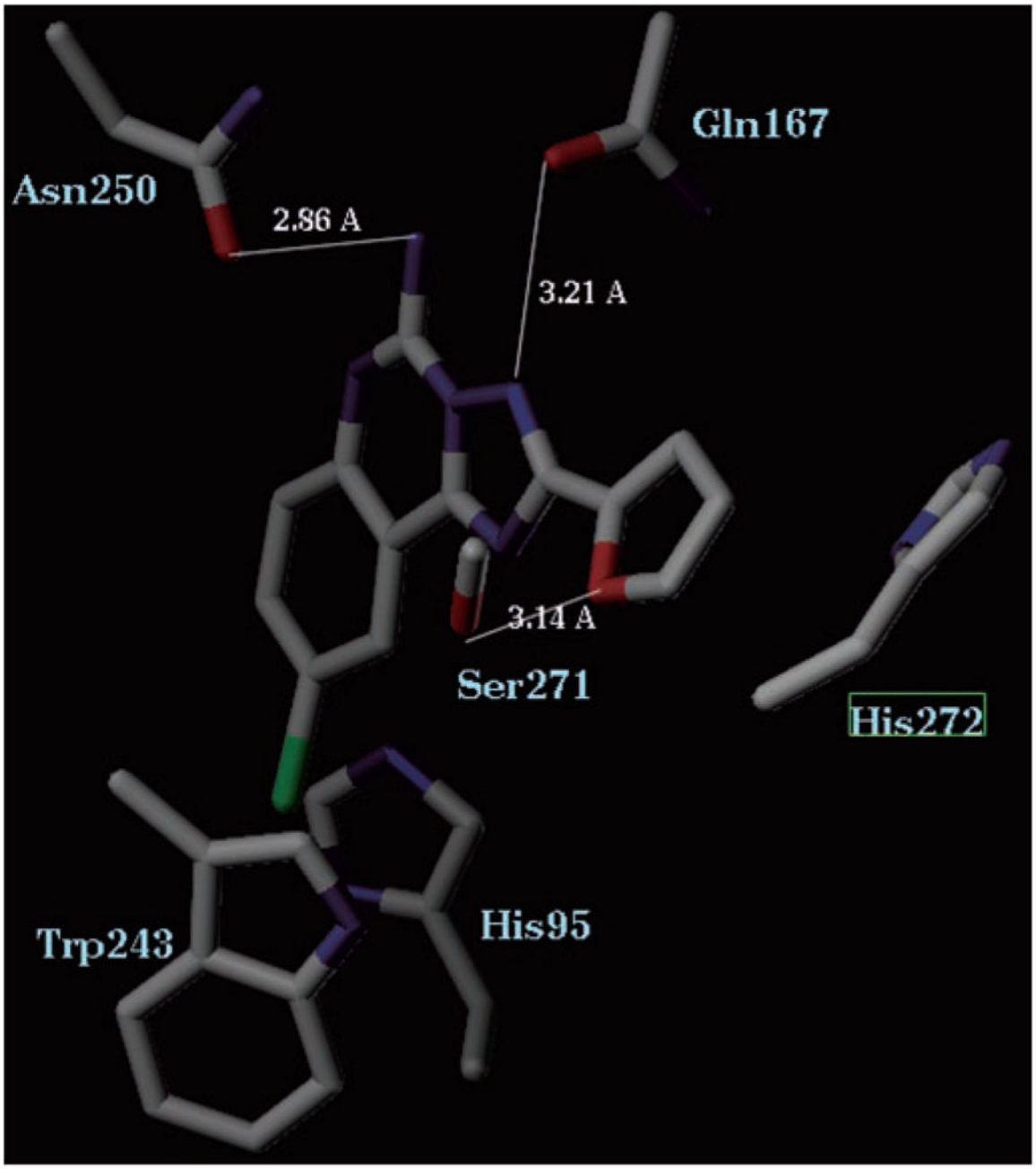

Fig. 8. Molecular model of the nonselective antagonist CGS15943 binding to the human A_3 adenosine receptor

Residues in proximity to this triazoloquinazoline are shown. *Blue*, nitrogen, *red*, oxygen, *green*, chlorine.

TABLE I

Affinities of various agonists and antagonists in binding experiments at WT and mutant human A_3 adenosine receptors

Binding parameters were measured on COS-7-transfected cells as described under "Experimental Procedures." The binding affinity of various ligands for different receptors was determined by using the agonist radioligand [^{125}I]I-AB-MECA (1.0 nM). Values represent the mean ± S.E. of at least three independent determinations. NA, no activity. A K_i value could not be determined (ND) for the N250A (6.55) mutant receptor, as this mutant receptor did bind to the agonist radioligand [^{125}I]I-AB-MECA or the antagonist radioligand [^{3}H]PSB-11.

	K_i (nM)								
	WT	**H95A (3.37)**	**K152A (EL2)**	**W243A (6.48)**	**W243F (6.48)**	**L244A (6.49)**	**S247A (6.52)**	**N250A (6.55)**	**H272E[a] (7.43)**
Agonists									
[^{125}I]I-AB-MECA (K_d)	1.7 ± 0.4	5.7 ± 1.2	3.7 ± 1.4	1.1 ± 0.3	1.6 ± 0.2	0.85 ± 0.11	1.7 ± 0.3	NA	ND
CADO	523 ± 116	58,200 ± 6500	323 ± 107	334 ± 67	321 ± 14	ND	927 ± 353	ND	11,600 ± 4200
NECA	249 ± 72	3430 ± 900	278 ± 44	166 ± 77	132 ± 45	68 ± 14	247 ± 60	ND	3200 ± 770
Cl-IB-MECA	2.3 ± 0.6	60 ± 15	1.7 ± 0.6	2.9 ± 0.5	1.9 ± 0.6	2.5 ± 0.7	2.2 ± 0.2	ND	20 ± 4
MRS1898	1.4 ± 0.4	143 ± 36	2.3 ± 0.6	2.1 ± 0.6	1.2 ± 0.3	0.73 ± 0.31	1.5 ± 0.5	ND	9.9 ± 2.6
DBXRM	2830 ± 570	36,300 ± 11,500	6030 ± 2320	4390 ± 950	2640 ± 530	7550 ± 2340	3040 ± 570	ND	ND
Antagonists									
CGS15943	182 ± 71	5130 ± 1140	571 ± 124	1160 ± 340	547 ± 87	209 ± 48	333 ± 144	ND	3260 ± 990
MRS1220	1.6 ± 0.3	976 ± 119	5.4 ± 0.7	45 ± 13	10.2 ± 3.3	0.63 ± 0.14	3.1 ± 1.4	ND	ND
VUF8504	68 ± 19	4000 ± 590	575 ± 134	2570 ± 690	1340 ± 370	42 ± 15	81 ± 26	ND	1690 ± 340
XAC	142 ± 35	9440 ± 3260	726 ± 214	552 ± 79	263 ± 46	61 - 18	165 - 47	ND	20,100 – 4500

[a]Data are from Jacobson *et al.* (21).

Table II

Examination of the influence of 2-chloro substitution on the effects of mutangenesis on agonist affinity

Agonist[a]	K_i, nM		K_I mutant/K_I WT for 2-H	2-Cl analogue
	WT	H95A		
Adenosine				111
IB-MECA	4.5 ± 1.6	44 ± 12	9.8	26
MRS1939	1.6 ± 0.3	147 ± 45	92	100

[a]The 2-H analogue is listed in this column. The corresponding 2-chloro analogues are CADO, Cl-IB-MECA, and MRS 1898, respectively. The binding affinity of adenosine is not measurable directly, due to the need to add ADA.